Article

New Quartz Oscillator Switching Method for Nano-Henry Range Inductance Measurements

Vojko Matko * and Karel Jezernik

Faculty of Electrical Engineering and Computer Science, University of Maribor, Smetanova 17, 2000 Maribor, Slovenia; E-Mail: karel.jezernik@uni-mb.si

* Author to whom correspondence should be addressed; E-Mail: vojko.matko@uni-mb.si;
Tel.: +386-2-220-7111; Fax: +386-2-220-7272.

Abstract: This article introduces a new method for nano-Henry inductance measurements at the frequency of 4.999 MHz with a single quartz crystal oscillating in the switching oscillating circuit. The real novelty of this method, however, lies in a considerable reduction of the temperature influence of AT-cut crystal frequency change in the temperature range between 0 °C and 50 °C through a switching method which compensates for the crystal's natural temperature characteristics. This allows for the compensation of any influences on the crystal such as the compensation of the non-linear temperature characteristics and the ageing of both the crystal and other oscillating circuit elements, as well as the reduction of the output frequency measurement errors with the help of an additional reference frequency. The experimental results show that the switching method greatly improves the measurement of small inductance changes in the range between μH and nH, allowing as a result high-precision measurements (~0.35 fH) in this range.

Keywords: nano-Henry range measurement of small inductance changes; switching oscillating method; compensation of quartz crystal temperature characteristics

1. Introduction

When using existing bridge methods for inductance measurement, one experiences the problem of the occurrence of stray capacitances and inductances once all bridge elements are connected. Also, the range of measurement is generally limited to just 100 kHz. In the Maxwell-Wien bridge, the

measurement range is between 20 Hz and 1 MHz and the relative error of measurement is about 0.1% of the measured values. The resonance methods, on the other hand, are based on the application of a series or parallel resonance LC circuits as elements of either a bridge circuit or a two-port (four-terminal) "T"-type network. A "double T" network can be used for inductive impedance measurements at high frequencies (up to 100 MHz; the relative error of measurement is about 0.1%). Proper design of LCR meters limits the influence of the factors causing error of measurement (*i.e.*, stray coupling and distortions). The results of inductance measurements also depend on how the measurements are performed, including how the measured inductor is connected to the meter. Care should be taken to limit such influences as inductive and capacitive coupling of the inductive element to the environment, sources of distortion, and the choice of operating frequency. One such precise LCR meter is also 4284A Hewlett-Packard meter, whose range of measurement is between 0.01 nH and 99.9999 kH in the frequency range 20 Hz–1 MHz with the basic accuracy of 0.05%. However, its price is relatively expensive ~$9,500 [1–6].

To improve the precision and sensitivity of small inductance change measurements using quartz crystals, a switching configuration has been made. Approaches described in articles to date [7–10] achieved greater precision through compensation of various influences from non-linear temperature characteristics to ageing and frequency measurement influences (errors). Sensitivity, on the other hand, was increased using various techniques such as frequency pulling with the prime aim of achieving high sensitivity in the nano-Henry range. However, the inequality of quartz crystal pair temperature characteristics has limited research in that direction [1].

Differential quartz crystal oscillating measurement methods typically consist of two oscillators using two quartz crystals (temperature pairs) [1,2,10,11], whereby these temperature pairs usually do not have ideal temperature characteristics. This means that the temperature compensation influence can be achieved only to a certain degree and only within a limited temperature range. The results of past experiments show that quartz crystal temperature characteristics are of primary importance in high-precision measurement of small inductances. Equally important are a stable electronic oscillating circuit supply voltage and the related quality of individual elements [1–6].

In cases where the oscillator housing is not hermetically closed, one should also take into account the influence of the outside environment on the outside oscillator elements. The key thing is to have these elements made of high-quality stable materials such as Al_2O_3, which is known for its very good temperature stability (coefficient of thermal expansion—$8.1 \times 10^{-6}/°C$, dielectric constant—9.1 (1 MHz), maximum working temperature—1,700 °C, hardness—1,175 Kg/mm^2, tensile strength—107 MPa, compressive strength—1,288 MPa, bending strength—248 MPa, porosity—0%,...) [10–13].

The research described in this article introduces a new idea which looks for ways to compensate the temperature characteristics of a single quartz crystal. The real novelty of this approach lies in the fact that AT-cut quartz crystals with various temperature characteristics can be used. Similarly, the aim is also to compensate the temperature influence of the measuring inductances on the quartz crystal oscillation frequency, the influence of the supply voltage on the oscillating circuit as well as the influence of any other electronic circuit element, and to foresee the differential functioning of the sensitive inductive elements [10,14,15].

Switching circuits may sometimes have some disadvantages, which can, however, be greatly minimized using appropriate approaches. In case of oscillator circuits, an oscillator with a good start-

up, *i.e.*, with a reliable crystal oscillation during the start and later on, is a must. We refer to this as short- and long-term frequency temperature stability. Dynamic stability during the temperature changes in the extended operating range is another factor of great importance [14–20].

Typical frequency measurement is limited to the counter capacities, *i.e.*, to the errors in a given frequency range. At higher frequency measurements, the heterodyne measurement method proves to be better. In this method, the frequency difference is transformed to a lower range, where it can be measured with a substantially higher precision than the original high frequency. For such measurements, instruments such as counter (HM 8122) are typically used [1,15,18].

There is also the problem of how to combine and implement high sensitivity (frequency pulling), linearize frequency inductance characteristics, set the crystal oscillation frequency working point, compensate other influences and ensure high temperature stability discussed by previous articles. The best frequency range to achieve high pulling sensitivity and stability for high quality crystals is between 3 and 10 MH. The problem of load pulling becomes worse at higher frequencies, because both the quality (Q) and isolation of the quartz crystal decrease. The frequency stability also decreases due to lower Q value [1,8,9,19–25].
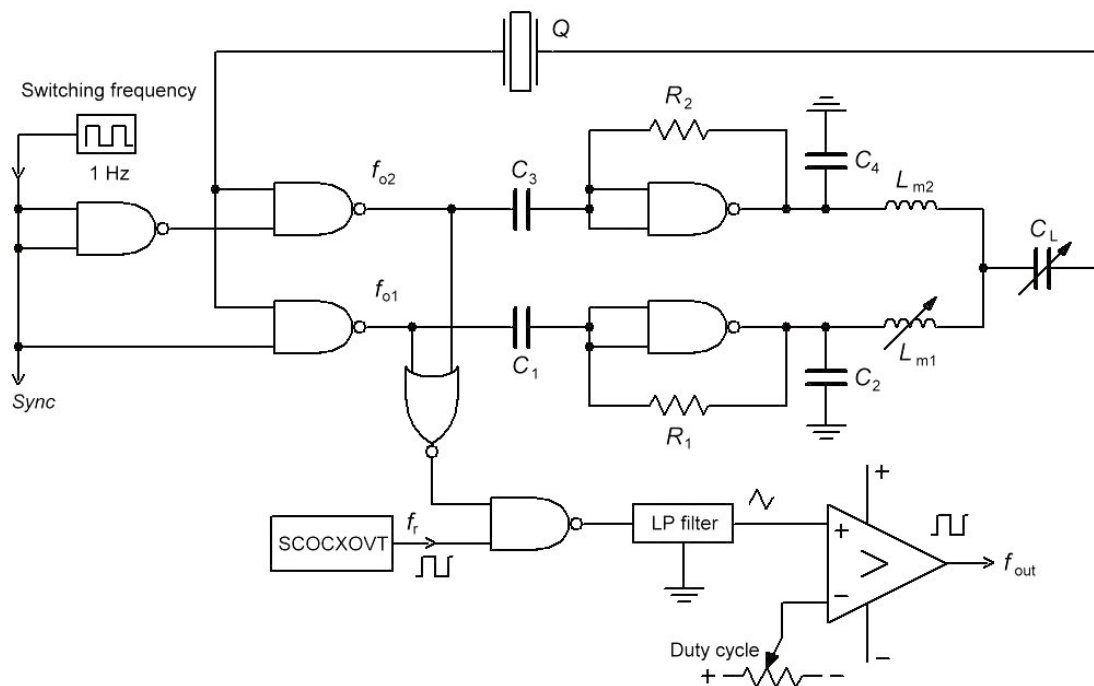
2. Dual Switching Mode Oscillator

A dual switching mode oscillator is based on one quartz crystal and a dual oscillator circuit with switching part together (Figure 1) [1,14,19]. The switching between the frequencies f_{o1} and f_{o2} is done by an additional switching frequency (*Sync*) of 1 Hz and an additional circuit of three NAND gates. Inductances L_{m1} and L_{m2} can also be used as sensors in differential mode. Inductors can be produced in various standard forms. They can generally be classified as strip inductors or spiral inductors. Straight sections of wires or strip are used for low inductance values, typically less than 10 nH, while spiral have higher quality Q_s and can provide higher inductance values. The presence of a ground plane also affects the inductance. The inductance decreases when the ground plane is brought nearer to the conducting line. Planar inductors are made essentially with a single-layer metallization scheme, in which a conducting layer is etched on a dielectric substrate. In the experiment, L_{m1} consists of two inductances in the series—standard element (123 µH) and straight sections of strip for low inductance values (2 nH) (etched on Al_2O_3). The inductance of a strip line can be written as [26–31]:

$$L_{straight} = 2l \left[ln\left(\frac{l}{w+t}\right) + 0.22\frac{w+t}{l} + 1.19 \right]$$ (1)

Where $L_{straight}$ is the segment inductance in nH, l = 0.5 cm, w = 0.05 cm, and t = 0.05 cm are the segment length, width and thickness, respectively. By changing the length l (using constant values), inductance values of $L_{straight}$ in the range between 0 and 2 nH can be set. Inductance $L_{straight}$ was measured by a HP 4194A impedance/gain-phase analyzer. Inductance L_{m2} has the value of 123 µH. The basic values of inductances L_{m1} and L_{m2} are determined with the compensation criterion (Equation (2)) in relation to the parasitic capacitance C_o = 8 pF of the quartz crystal [1,8,19,26]:

$$k{\cdot}L_m = 1/k{\cdot}C_0$$ (2)

Figure 1. Dual switching mode oscillator.

The two inductances L_{m1} and L_{m2} play the roles of sensor and compensation elements at the same time, which is another of the novelties introduced by this method. Capacitance C_L is used for the simultaneous fine tuning of the frequencies f_{o1} and f_{o2}. The compensation factor k can be set with the fixed values L_{m1} and L_{m2} [7,8,26,27].

The signal corresponding to the difference between the frequencies enters the LP filter. At the LP filter output, the triangular signal is produced which is then converted with the help of a comparator to a rectangular signal representing the output signal. The output f_{out} thus represents the output frequency signal which is synchronously measured with regard to the switch of signal *Sync*. Capacitances C_2 and C_4 serve to suppress the spurious responses to avoid crystal oscillation at higher and/or lower frequencies [19,20,32]. Depending upon the sensor design and configuration, the spurious response modes should be weaker than the fundamental mode. The only thing is that they are taking away the energy from the mode of interest. In the oscillator circuit, the inductances L_{m1} and L_{m2} are in series with the quartz crystal and together with the compensation method (C_0) increase and linearize the frequency pulling range [8,9]. When inductances L_{m1} and L_{m2} are the same, f_{out} remains the same at state 1 and 0 of *Sync* signal and depends on the quartz crystal resonant frequency f_0, quartz crystal temperature characteristics $\Delta f(T)$, its ageing $\Delta f(t)$ and the ΔC_L change. However, when the inductances L_{m1} and L_{m2} are different, the frequency f_{out} depends on the quartz crystal resonant frequency f_0, quartz crystal temperature characteristics $\Delta f(T)$, its ageing $\Delta f(t)$, and the ΔC_L or ΔL_{m1} change. In case of the difference of the two frequencies f_{o1} in f_{o2}, $\Delta f(T)$, ΔC_L and $\Delta f(t)$ are compensated because only one quartz characteristics is involved [14,19,20].

The output frequencies f_{out} depend on *Sync* signal and can be expanded to [14]:

$$f(Sync) - f_r = f_0 + \Delta f(T) + \Delta f(t) + \Delta C_L + \Delta f(counter\ error) + \Delta f(L_{m1}) + \Delta f(\Delta L_{m1}) - f_r \qquad (3)$$

$$f(\overline{Sync}) - f_r = f_0 + \Delta f(T) + \Delta f(t) + \Delta C_L + \Delta f(counter\ error) + \Delta f(L_{m2}) - f_r \qquad (4)$$

when joining f_0 and $\Delta f(L_{m1} + \Delta L_{m1})$, we get Equation (5). The particularity of this equation lies in the fact that it takes into account the compensation C_0 and at the same time linearizes the quartz characteristics due to the ΔL_{m1} change (Figure 1) and allows for the sensitivity setting [14,19,20].

$$f(Sync, k, \Delta L_{m1}) = \frac{1 + \dfrac{C}{2\left(\dfrac{1}{k}C_0 - \dfrac{1}{\omega_0{}^2 \cdot k \cdot (L_{m1} + \Delta L_{m1}) - \dfrac{1}{C_L}}\right)}}{2\pi \cdot \sqrt{L \cdot C}} + \Delta f(T) + \Delta f(t) + \Delta f(counter\ error) \tag{5}$$

where:

k_1, k_2, k_3—pulling sensitivity value [8],

L and C—mechanical behavior of the crystal element [8,33–36],

L_{m1}—measurement and compensation inductance 1 [33–36],

L_{m2}—compensation inductance 2,

C_0—parasitic capacitance of the crystal element and holder [8,33–36],

f_0—quartz crystal series resonant frequency [8,33–36],

T—temperature,

t—time.

$$\omega_0 = 2 \cdot \pi \cdot f_0 \tag{6}$$

when joining f_0 and $\Delta f(L_{m2})$, we get Equation (7) [10,14]:

$$f(\overline{Sync}, k, L_{m2}) = \frac{1 + \dfrac{C}{2\left(\dfrac{1}{k}C_0 - \dfrac{1}{\omega_0{}^2 \cdot k \cdot (L_{m2}) - \dfrac{1}{C_L}}\right)}}{2\pi \cdot \sqrt{L \cdot C}} + \Delta f(T) + \Delta f(t) + \Delta f(counter\ error) \tag{7}$$

The pulling sensitivity in Equations (5) and (7) can be set with the value k, achieving at the same time simultaneous dependence linearization $\Delta f(L_{m1} + \Delta L_{m1})$ [7,8]. At every switch between $Sync$ and $\overline{Sync}$, the frequency f_{out} is measured by counter and its value is transferred to the LabVIEW software calculating the difference between the two frequencies. The switching from $Sync$ to $\overline{Sync}$ also compensates the auxiliary frequency f_r, and consequently its frequency temperature stability as well. We get the frequency difference representing the temperature compensated and linear value of the frequency, which depends uniquely on the ΔL_{m1} change:

$$(f(Sync, k, L_{m1} + \Delta L_{m1}) - f_r) - (f(\overline{Sync}, k, L_{m2}) - f_r) = \Delta f(\Delta L_{m1}) \tag{8}$$

This means that it is neither dependent on the quartz crystal temperature characteristics $\Delta f(T)$ nor its ageing $\Delta f(t)$ and nor the circuit temperature characteristics influences (Equations (8) and (9)) [1,8,14]:

$$\Delta f(\Delta L_{m1}) = \frac{\dfrac{C}{2\left(\dfrac{1}{k}C_0 - \dfrac{1}{\omega_0{}^2 \cdot k \cdot (L_{m1} + \Delta L_{m1}) - \dfrac{1}{C_L}}\right)}}{2\pi \cdot \sqrt{L \cdot C}} - \frac{1 + \dfrac{C}{2\left(\dfrac{1}{k}C_0 - \dfrac{1}{\omega_0{}^2 \cdot k \cdot (L_{m2}) - \dfrac{1}{C_L}}\right)}}{2\pi \cdot \sqrt{L \cdot C}} \tag{9}$$

While the specified counter accuracy (HM 8122—option HO 85) $\pm 5 \times 10^{-9}$ does not allow for high-precision measurements of small output frequency changes at 4.999 MHz, the use of an additional reference frequency f_r = 4.999 MHz (auxiliary OCOCXOVT oscillator, Figure 1), of the frequency difference method (AND gate) and of the low pass filter enables precise measurements of the frequency difference between the switches *Sync* and $\overline{Sync}$ [18].

3. Quartz Temperature Characteristics Compensation

When using AT-cut crystals for high-precision measurements, a frequency change in the oscillation (up to 1 Hz) of the crystal can be detected in the range between 10 °C and 40 °C [1,14,19–37]. Generally, the different temperature frequency curves are represented as the cubical parabola with temperature inflection point lying between 25 °C and 35 °C, depending on the crystal cut angle and the mechanical construction. The new method (Figure 1) allows the AT-cut crystal temperature characteristics compensation (under 1 Hz) through switching mode method, which compensates this characteristics and reduces its influence to a minimum [14,20,37–39].

In comparison to AT-cut crystals, NLSC-cut crystals are less sensitive to mechanical and thermal stress and provide lower aging and higher Q. Moreover, they are also less sensitive to drive levels. On the other hand, they require an oven, do not operate well at ambient temperatures as the frequency rapidly falls off at lower temperatures. However, since their inflection point is between 85 °C and 95 °C, it is very suitable for ovenized oscillators because a top around 90 °C leads to very low dependency of frequency against temperature [40]. Nevertheless, NLSC-cut crystals have a number of disadvantages, e.g., the motional capacitance is several times less than that of an AT of the same frequency, thus reducing the ability to "pull" the crystal frequency. They are also sensitive to electric fields and their cost is relatively high compared to AT-cut crystals [41–43].

4. Frequency Variation of Oscillator as Function of Time

Frequency variation of oscillator as function of time is normally considered in short-term stability (second-to-second temperature characteristics) and long-term stability over years. The short-term stability of a quartz crystal depends on the actual oscillator design and is totally controlled by the quartz crystal at low drive levels. Long-term stability (ageing) is naturally greater during the first part of the life of the crystal unit. The ageing rates of the best cold weld crystals are less than ±1 ppm/year (10 °C to 40 °C) [1,19,32,38,39]. The ageing of other electronic circuit elements is compensated in the same way.

5. Output Frequency Measurement Error

Typical counter (HM 8122—option HO 85) accuracy is $\pm 5 \times 10^{-9}$ (through the entire working temperature range 10 °C up to 40 °C), in 5×10^{-9}/day after 48 h continuous operation with crystal oven controlled (OCXO) [18]. The novel switching method highly reduces the influence of the short- and long-term stability of the above described counter due to the compensation of previously mentioned influences of a single quartz crystal and the circuit as well as the influence of the difference method using additional reference frequency f_r = 4.999 MHz. Frequency f_r is produced by oven

controlled crystal oscillator (OCOCXOVT) with a short-term stability (0.1 to 30 s) 1×10^{-10} in the temperature range between 0 °C and 60 °C following the warm-up time of 30 min [17,18,38,39].

6. Experimental Results

For this research, the quartz switching oscillator circuit (Figure 1) was experimentally selected switching between inductances L_{m1} and L_{m2} with the frequency of 1 Hz. The L_m values were in the range between 122 µH and 124 µH. Within 1 s time, the HM 8122 external counter measured (using LabVIEW software) both frequencies $(f(Sync, k, L_{m1} + \Delta L_{m1}) - f_r)$ and $(f(\overline{Sync}, k, L_{m2}) - f_r)$ at the output f_{out}.

In Table 1, f_0 represents the fundamental mode quartz crystal resonant frequency. R, L, C, C_0, are quartz crystal equivalent circuit elements (Q_q is quality) [1,2,7,8,32]. The experimental quartz data values in the quartz crystal equivalent circuit were measured by Jauch [32]. L_{m1} and L_{m2} were measured using the HP 4194A impedance/gain-phase analyzer.

Table 1. Quartz data [32].

f_0 (MHz)	R(Ohm)	L(mH)	C(fF)	C_o(pF)	Q_q	L_{m1}(µH)	L_{m2}(µH)
4.999	10	41	25	8	127,800	122.75–123.75	123.75

Figure 2. Quartz crystal sensitivity and linearity for k = 0.5, 1, 2 for $L_{m1} + \Delta L_{m1}$ and L_{m2} = 123.75 µH $\cdot k$, C_L = 22 nF.
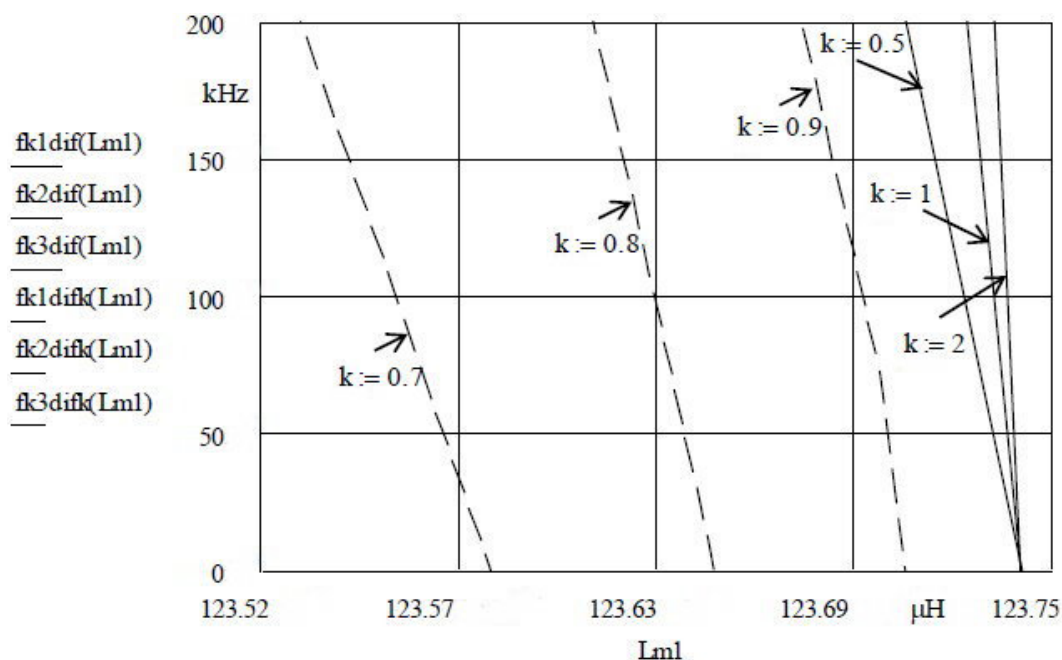

Figure 2 illustrates the change of inductance values. L_{m1} changes for ΔL_{m1} with the criterion k at the constant capacitance value C_L = 22 nF. Simultaneously with L_{m1}, the inductance L_{m2} = 123.75 µH is changed with the same criterion k (Equation (7)). Figure 2 does not display the inductance L_{m2} because in relation to k it has a fixed value depending on k. ΔL_{m1} changes with the change of the length l (Equation (1)) [26–31], and is measured by a HP 4194A impedance/gain-phase analyzer. Figure 2 shows that various frequency sensitivities with the intersection at L_{m1} = 123.742 µH (due to different k)

are produced. Factor k relates to the compensation criterion C_0 [8]. This means that if we simultaneously change k ($k_1 = 0.5$, $k_2 = 1$, $k_3 = 2$), the size of the frequency sensitivity of $L_{m1} + \Delta L_{m1}$ can be determined with the frequency difference $f(Sync) - f(\overline{Sync})$ for ($f_{k1dif}(L_{m1})$, $f_{k2dif}(L_{m1})$, $f_{k3dif}(L_{m1})$).

Figure 2 also shows that by changing the inductance values of L_{m1} alone with the values of the criterion $k = 0.7$, 0.8, 0.9 at the constant capacitance value $C_L = 22$ nF and $k = 1$ for fixed $L_{m2} = 123.75$ µH in all three cases, the oscillator frequency can be set to the left and to the right of the initially set frequency by changing the value of k for L_{m1} alone.

Figures 3 illustrates stepwise capacitance value changes $C_L = 3.3$ nF, 10 nF and 100 nF at constant compensation factors k for inductances L_{m1} and $L_{m2} = 123.75$ µH. One can see that the capacitance C_L can also be used to set the sensitivity (inclination).

Figure 3. Quartz crystal sensitivity for different k for L_{m1} and different C_L.
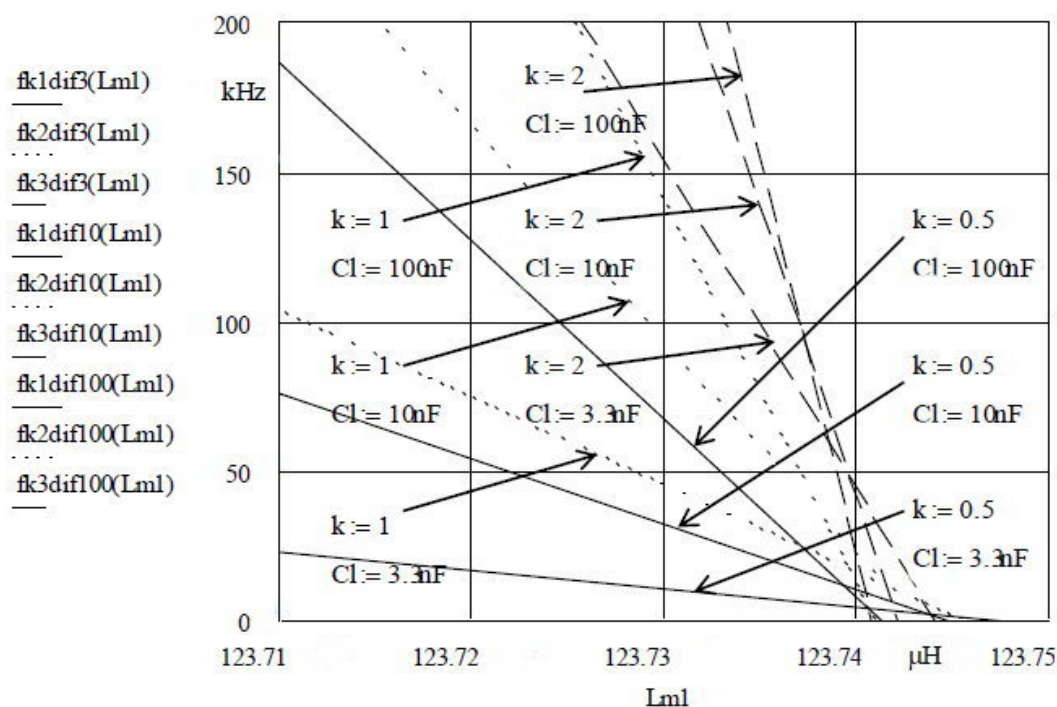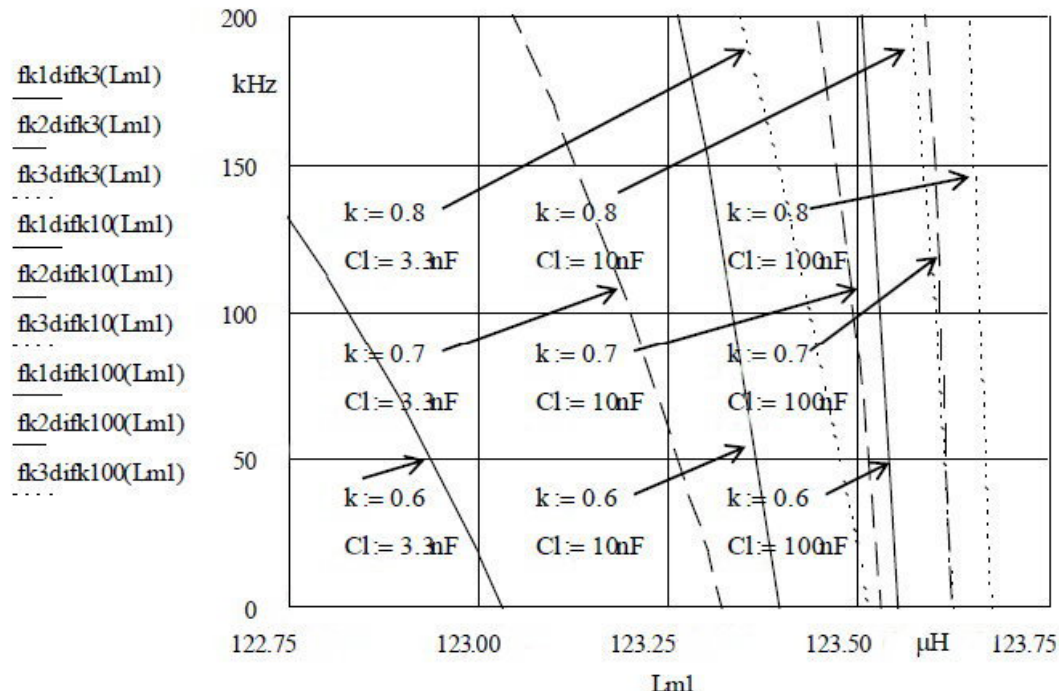

Figure 4 shows that stepwise change of k (0.6, 0.7, 0.8) for L_{m1} and constant values $k = 1$ for $L_{m2} = 123.75$ µH (for all cases) can change the set oscillator frequency (and to a certain degree the sensitivity as well) by changing the capacitance $C_L = 3.3$ nF, 10 nF and 100 nF.

The experimentally selected k value combinations show that with the above C_L values and the compensation ratio k for C_0, crystal oscillation frequency (oscillator frequency), sensitivity and linearity with simultaneous compensation of disturbing influences can be set. The pulling sensitivity is the highest at the value $k = 2$ (Figure 3) while the stability is lower. At values $k = 0.5$ the frequency stability is better, however the pulling sensitivity is lower. The highest sensitivity (~70 nH/200 kHz) is shown in Figure 4. For the temperature range between 0 °C and 50 °C [14,18], the experimentally measured results of the frequency changes (Programmable Counter/Timer HM 8122) were ±0.00001 Hz (second-to-second stability) and ±0.0001 Hz (minute-to-minute stability) which makes the high-precision measurement of nH changes possible in a given temperature range [14–18,44]. At the highest

sensitivity of ~70 nH/200 kHz at ±0.0001 Hz (minute-to-minute stability), the measurement precision is ~0.35 fH.

Figure 4. Quartz crystal frequency shift for $k = 0.6, 0.7, 0.8$ for L_{m1} and different C_L.

The results illustrated in Figures 2 to 4 provide a comparison of inductance changes L_{m1} in the frequency range 0 to 200 kHz. One can observe non-linear changes which occur due to the width of frequency range. The non-linearity of these frequency characteristics depends upon the choice of individual values of the compensation factor k and the value of the capacitor C_L.

Figure 5. Frequency stability ($f(Sync, k, L_{m1}) - f_r$) occurring when changing the temperature in the range 0–50 °C (measurement time 2.5 h—two cycles).

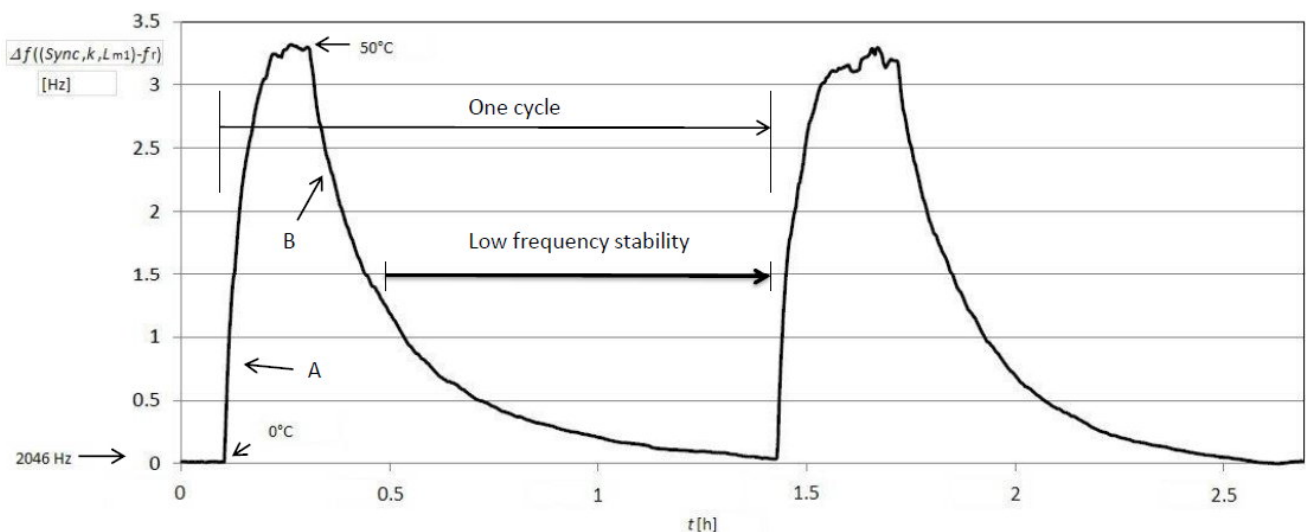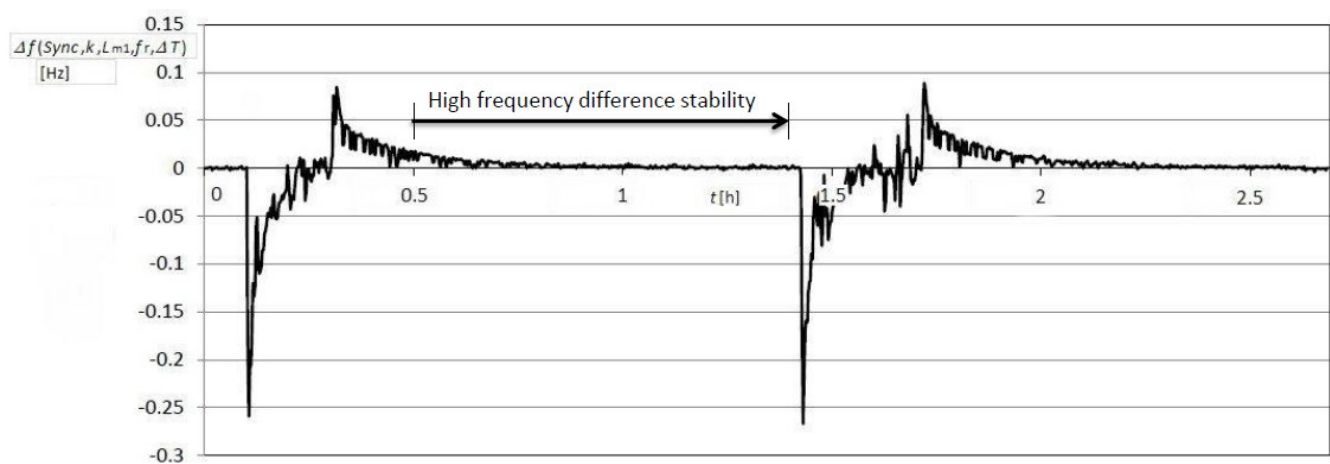Figure 5 shows the frequency stability ($f(Sync, k, L_{m1}) - f_r$) (at the beginning of temperature cycling the stable frequency was 2,064 Hz at 0 °C) occurring when changing the temperature in the

range between 0 °C and 50 °C at the state *Sync* and fixed value $L_{ml} = 123.65$ µH (Figure 4). The crystal used in the experiment was AT-cut (cut angle: 0`) [37] quartz crystal with temperature change ±5 ppm in the range 10 °C–30 °C. The A and B areas illustrate dynamic change of frequency at the temperature change ranging from 0 °C to 50 °C and back to 0 °C.

Figure 6 illustrates frequency stability $\Delta f(L_{m1})$ (Equation (8)) during the change of temperature in the range 0 °C–50 °C at the fixed value $L_{ml} = 123.65$ µH (Figure 4) once both frequencies are deducted $(f(Sync, k, L_{m1} + \Delta L_{m1}) - f_r) - (f(\overline{Sync}, k, L_{m2}) - f_r)$. Deduction of both frequencies in relation to Sync signal is performed by LabVIEW software. In addition, this Figure also illustrates the temperature compensation of the quartz crystal natural temperature characteristics.

Figure 6. Frequency difference stability $(f(Sync, k, L_{m1} + \Delta L_{m1}) - f_r)$ $-(f(\overline{Sync}, k, L_{m2}) - f_r)$ at the change of temperature in the range 0 °C–50 °C (measurement time 2.5 h—two cycles).

The comparison of results in Figures 5 and 6 points to dynamic frequency stability change (Figure 6) and to the high stability (high frequency difference stability— ±0.01 Hz) area when the temperature changes less quickly.

7. Conclusions

This article discusses the results of the research aimed at the reduction of the temperature influence of the AT-cut crystal frequency change using the sensor switching method for the inductance change measurement in the nH range. These results show that the use of the dual oscillator switching method excellently compensates quartz crystal non-linear frequency-temperature characteristics, its ageing and oscillator circuit elements. For this purpose AT-cut crystals were used. The value of inductance ΔL_{m1} is set by its length and it is produced as a strip line etched on Al_2O_3. Basic inductance values L_{m1} and L_{m2} are two identical elements. The article provides possible oscillator frequency, sensitivity and linearity settings with the compensation factor k, the frequency setting (working point) with the capacitance value C_L, the temperature compensation of the crystal characteristics and those of other elements as well as frequency stability after temperature compensation. Also taken into account have been past sensitivity and linearity studies (listed in the references). The great advantage of this method is that it resolves the issue of the sensitivity, linearity and crystal oscillation working point setting as well as the

problem of crystal natural temperature characteristics compensation at the same time. The results shown in the article relate to a significantly wider frequency range (0–200 kHz) than is usually covered by practical measurements. With the help of an additional reference frequency and inductance, which makes the differential measurement of inductance changes possible, the output frequency errors can be greatly reduced due to the fact that the frequency counter measures in the range of a few kHz with greater accuracy (more decimal points). The frequency difference in relation to *Sync* signal and the temperature crystal compensation is calculated with the help of the *Sync* signal and the LabVIEW software (Figure 6). This makes this switching method a very interesting tool for the measurement of inductance and small inductance changes which is highly demanded in the sensor industry. The mode of compensation used for the AT-cut crystals opens possibilities for its application in other crystal cuts.

The factors affecting frequency stability such as wide operating temperature range, the use of various types of crystals and drive level should also be considered because a stable oscillator circuit is of vital importance. Stability of the electronic circuit depends upon the circuit type and quality of its elements (elements of the same values must be of the same producer and of the same quality). It is also important that the drive level of the quartz crystal does not exceed 20 μW [15,19,20,32]. These results clearly show that the dual switching method for high-precision small inductance change measurements opens up new possibilities for such measurements compensating at the same time temperature characteristic and other disturbing influences. This makes this new method highly promising for nH range measurements in various fields of physics, chemistry, mechanics, biosensor technology, atomic force, *etc*.

References

1. Webster, J.G. *The Measurement, Instrumentation, and Sensors Handbook, Inductance Measurement*; CRC Press: Boca Raton, FL, USA, 1999; pp. 1–13.
2. Bentley, J.P. *Principles of Measurement Systems*, 2nd ed.; John Wiley & Sons: New York, NY, USA, 1988.
3. Helfrick, A.D.; Cooper, W.D. *Modern Electronic Instrumentation and Measurement Technique*; Prenice-Hall: Englewood Cliffs, NJ, USA, 1990.
4. Jones, L.D.; Chin, A.F. *Electronic Instruments and Measurements*, 2nd ed.; Prenice-Hall: Englewood Cliffs, NJ, USA, 1991.
5. Sydenham, P.H. *Handbook of Measurement Science*; John Wiley & Sons: New York, NY, USA, 1982; Volume 1.
6. Sydenham, P.H. *Handbook of Measurement Science*; John Wiley & Sons: New York, NY, USA, 1983; Volume 2.
7. Matko, V.; Jezernik, K. Greatly improved small inductance measurement using quartz crystal parasitic capacitance compensation. *Sensors* **2010**, *10*, 3954–3960.
8. Matko, V.; Šafarič, R. Major improvements of quartz crystal pulling sensitivity and linearity using series reactance. *Sensors* **2009**, *9*, 8263–8270.
9. Matko, V. Comparison of frequency pullability in oscillators using a single AT-cut quartz crystal and those using two single AT cut crystals connected in parallel with a series load capacitance or series load inductance. *Sensors* **2006**, *6*, 746–755.

10. Kusters, J.A.; Vig, J.R. Thermal hysteresis in quartz resonators. In *Proceedings of the 44th Annual Symposium on Frequency Control*, Baltimore, MD, USA, 23–25 May 1990; pp. 165–175.

11. Nihon Dempa Kogyo Co., Ltd. OCXO 9150At. Available online: http://www.datasheetarchive.com/915-datasheet.html (accessed on 7 February 2012).

12. *CRC Handbook of Chemistry and Physics*, 77th ed.; CRC Press: Boca Raton, FL, USA, 1995.

13. Accuratus, Aluminum Oxide. Al_2O_3 Material Characteristics. Available online: http://accuratus.com/alumox.htmla (accessed on 7 February 2012).

14. Matko, V. Next generation AT-cut quartz crystal sensing device. *Sensor* **2011**, *11*, 4474–4482.

15. Rutman, J.; Walls, F.L. Characterization of frequency stability in precision frequency sources. *IEEE Trans. Instrum. Meas.* **1991**, *79*, 952–960.

16. ATMEL. Analyzing the Behavior of an Oscillator and Ensuring Good Start-Up. Available online: http://www.atmel.com/dyn/resources/prod_documents/doc4363.pdf (accessed on 7 February 2012).

17. *Oscillator Start-Up Time*; Note AN97090; Philips Electronics: Eindhoven, The Netherlands, 2001.

18. *Specification of HM8122*; Hameg Instruments: Mainhausen, Germany, 2008.

19. Euroquartz, Quartz Oscillator Theory. Available online: http://www.euroquartz.co.uk (accessed on 7 February 2012).

20. Stanford Research Systems, Quartz Crystal Microbalance Theory. Available online: http://www.thinksrs.com/downloads/PDFs/ApplicationNotes/QCMTheoryapp.pdf (accessed on 7 February 2012).

21. Bechmann, R. Single response thickness-shear mode resonators using circular bevelled plates. *J. Sci. Instrum.* **1952**, *29*, 73–76.

22. Walls, F.L.; Vig, J.R. Fundamental limits on the frequency stabilities of crystal oscillators. *IEEE Trans. Ultrason. Ferroelectr. Freq. Control* **1995**, *42*, 576–589.

23. Lu, F.; Lee, H.P.; Lim, S.P. Energy-trapping analysis for the bi-stepped mesa quartz crystal microbalance using the finite element method. *Smart Mater. Struct.* **2005**, doi: 10.1088/0964-1726/14/1/028.

24. Janshoff, A.; Galla, H.J.; Steinem, C. Piezoelectric mass-sensing devices as biosensors—An alternative to optical biosensors*? Angew. Chem. Int. Ed.* **2000**, *39*, 4004–4032.

25. Kao, P.; Allara, D.; Tadigadapa, S. Fabrication and performance characteristics of high-frequency micromachined bulk acoustic wave quartz resonator arrays. *Meas. Sci. Technol.* **2009**, doi: 10.1088/0957-0233/20/12/124007.

26. Vijay, K.; Vinoy, K.J.; Jose, K.A. *MEMS Inductors and Capacitors. RF MEMS and Their Applications*; John Wiley & Sons: New York, NY, USA, 2003; pp. 183–240.

27. Bahl, I.J.; Bhartia, P. *Microwave Solid-State Circuit Design*; John Wiley & Sons: New York, NY, USA, 1998.

28. Greenhouse, H.M. Design of planar rectangular microelectronic inductors. *IEEE Trans. Parts Hybrids Packag.* **1974**, *10*, 101–109.

29. Konishi, Y. *Microwave Integrated Circuits*; Marcel Dekker: New York, NY, USA, 1991.

30. Yamaguchi, M.; Mastumo, M.; Ohzeki, H.; Arai, K.I. Fabrication and basic characteristics of dry-etched micro inductors. *IEEE Trans. Magnet.* **1990**, *26*, 2014–2016.

31. Yamaguchi, M.; Mastumo, M.; Ohzeki, H.; Arai, K.I. Analysis of the inductance and the stray capacitance of the dry-etched micro inductors. *IEEE Trans. Magnet.* **1991**, *27*, 5274–5275.

32. Jauch Quartz GmbH. *Quartz Crystal Theory*. Available online: http://www.jauch.de/ablage/med_00000619_1193753698_Quartz%20Crystal%20Theory%202007.pdf (accessed on 7 February 2012).

33. Bandey, H.L.; Martin, S.J.; Cernosek, R.W.; Hillman, A.R. Modeling the responses of thickness-shear mode resonators under various loading conditions. *Anal. Chem.* **1999**, *71*, 2205–2214.

34. Voinova, M.V.; Rodahl, M.; Jonson, M.; Kasemo, B. Viscoelastic acoustic response of layered polymer films at fluid-solid interfaces: Continuum mechanics approach. *Phys. Scr.* **1999**, doi: 10.1238/Physica.Regular.059a00391.

35. Martin, S.J.; Granstaff, V.E.; Frye, G.C. Characterization of a quartz crystal microbalance with simultaneous mass and liquid loading. *Anal. Chem.* **1991**, *63*, 2272–2281.

36. Granstaff, V.E.; Martin, S.J. Characterization of a thickness-shear mode quartz resonator with multiple nonpiezoelectric layers. *J. Appl. Phys.* **1994**, *75*, 1319–1329.

37. Vig, J.R. *Quartz Crystal Resonators and Oscillators, For Frequency Control and Timing Applications*; SLCET-TR, 88–1 (Rev.8.4.2), AD-A328861; U.S. Army Communications-Electronics Command: Fort Monmouth, NJ, USA, 2000; pp. 4–43.

38. Golledge. Frequency Control Products. Available online: http://www.golledge.com/docs/products/ocxos/ocxos_pcb.htm (accessed on 7 February 2012).

39. Lap-Tech Inc. Standard Frequency Components. Available online: http://www.laptech.com/ (accessed on 7 February 2012).

40. Gufflet, N. Quartz *Crystal Resonators*; KVG Quartz Crystal Technology GmbH: Heidelberg, Germany, 2011; p. 8.

41. Vectron international. Oven Controlled Crystal Oscillators. Available online: http://www.ofc.com/ products/ocxo/ocxos.htm (accessed on 7 February 2012).

42. Kahan, A. Cut Angles for Quartz Crystal Resonators. U.S. Patent 4,499,395, 12 February 1985.

43. Kruse, P.W. Skatrud, D.D. *Uncooled Infrared Imaging Arrays and Systems, Quartz Microresonators as Infrared Sensors*; Academic Press: San Diego, CA, USA, 1997; p. 273.

44. Behling, C. The Non Gravimetric Response of Thickness Shear Mode Resonators for Sensor Applications. Ph.D. Thesis, Otto-von-Guericke University, Magdeburg, Germany, 1999.